Report

Apollo, an Artemis-Related Nuclease, Interacts with TRF2 and Protects Human Telomeres in S Phase

Megan van Overbeek[1] and **Titia de Lange**[1,*]
[1] Laboratory for Cell Biology and Genetics
The Rockefeller University
1230 York Avenue
New York, New York 10021

Summary

Human chromosome ends are protected by shelterin, an abundant six-subunit protein complex that binds specifically to the telomeric-repeat sequences, regulates telomere length, and ensures that chromosome ends do not elicit a DNA-damage response (reviewed in [1]). Using mass spectrometry of proteins associated with the shelterin component Rap1, we identified an SMN1/PSO2 nuclease family member that is closely related to Artemis [2]. We refer to this protein as Apollo and report that Apollo has the ability to localize to telomeres through an interaction with the shelterin component TRF2. Although its low abundance at telomeres indicates that Apollo is not a core component of shelterin, Apollo knockdown with RNAi resulted in senescence and the activation of a DNA-damage signal at telomeres as evidenced by *t*elomere-dysfunction-*i*nduced *f*oci (TIFs). The TIFs occurred primarily in S phase, suggesting that Apollo contributes to a processing step associated with the replication of chromosome ends. Furthermore, some of the metaphase chromosomes showed two telomeric signals at single-chromatid ends, suggesting an aberrant telomere structure. We propose that the Artemis-like nuclease Apollo is a shelterin accessory factor required for the protection of telomeres during or after their replication.

Results and Discussion

Shelterin associates with several accessory factors that are distinguished from the shelterin core components (TRF1, TRF2, Rap1, TIN2, TPP1, and POT1) on the basis of their lower abundance at telomeres and/or their transient association with chromosome ends [1]. Most shelterin-associated factors have additional nontelomeric functions, contributing to the DNA-damage response or other chromosomal transactions. We previously reported on mass spectrometry of nuclear proteins associated with a FLAG-[HA]2-tagged version of the TRF2-interacting factor Rap1 [3]. In the course of these experiments, a protein migrating slightly faster than Rap1 was reproducibly observed. However, identity of this Rap1-associated protein remained elusive, possibly because of its low abundance and/or the technique used for the polypeptide isolation, which involved slicing an entire gel lane into 2 mm pieces [3]. Therefore,

we repeated the isolation of the Rap1 complex to excise the 60 kDa band for mass spectrometry (Figure 1A). The Rap1/TRF2 complex was prepared under high-salt conditions, which abrogate the DNA binding activity of TRF2 and also diminishes the interaction between TRF2 and TIN2 [3], explaining why the Rap1 complex isolated in this manner contains relatively little TIN2 and the shelterin components that associate with TRF2/Rap1 through TIN2 (TRF1, TPP1, and POT1) (Figure 1A).

Mass spectrometry of the 60 kDa Rap1-associated protein identified six peptides from SNM1B (Figure 1A). SNM1B is one of three SNM1 genes in the mammalian genome that were identified on the basis of their sequence similarity to the *Saccharomyces cerevisiae* DNA interstand cross-link (ICL) repair gene PSO2/SNM1 [4]. PSO2 and its mammalian orthologs have metallo-β-lactamase/β-CASP domains [5, 6]. Although their functions have not been fully worked out, both SNM1A and B have been implicated in ICL repair [4, 7], and SNM1A localizes to sites of DNA damage generated by ionizing radiation (IR) [8]. SNM1C is known as Artemis, the nuclease involved in V(D)J recombination and whose deficiency leads to one form of SCID [2, 9, 10]. Artemis is also implicated in nonhomologous end joining (NHEJ) of IR-induced DNA breaks [11], and Artemis-deficient mouse cells are radiosensitive, showing an increased level of IR-induced genome instability [12]. SNM1C and SNM1B are more closely related to each other than to SNM1A (Figure S1A in the Supplemental Data available online). To emphasize the relatedness of SNM1B and Artemis, we refer to this protein as Apollo, the twin brother of Artemis in Greek mythology.

The association of Apollo with shelterin was verified on the basis of recovery of endogenous shelterin components in immunoprecipitates (IPs) of transiently transfected Myc-tagged Apollo. Myc-Apollo brought down TRF2 and Rap1 but not TIN2 or TRF1 (Figure 1B). Apollo IPs cotransfected with individual shelterin components showed an association of Apollo with TRF2 and Rap1, whereas the recovery of Apollo in association with TRF1, TIN2, and POT1 was minimal (Figure 1C). In order to determine whether Apollo could associate with TRF2 and to what extent Rap1 contributed to the interactions, we cotransfected Apollo with several TRF2 truncation alleles. These experiments indicated that Apollo can associate with TRF2's TRFH (TRF homology [13, 14]) region, which is a protein-protein interaction domain that mediates homodimerization of TRF2 (Figures 1D and 1E). Given that the TRFH domain is not sufficient for the interaction of TRF2 with Rap1 [15], these results imply that the Apollo-TRF2 interaction is likely to be Rap1 independent. The co-IP of Apollo and Rap1 (Figures 1B and 1C) is probably due to the efficient association of Rap1 with endogenous TRF2. In the course of these experiments, we also found that Apollo had the ability to interact with itself, resulting in coimmunoprecipitation of Myc-tagged and HA-tagged Apollo (Figure 1F). These results suggest that Apollo associates with shelterin

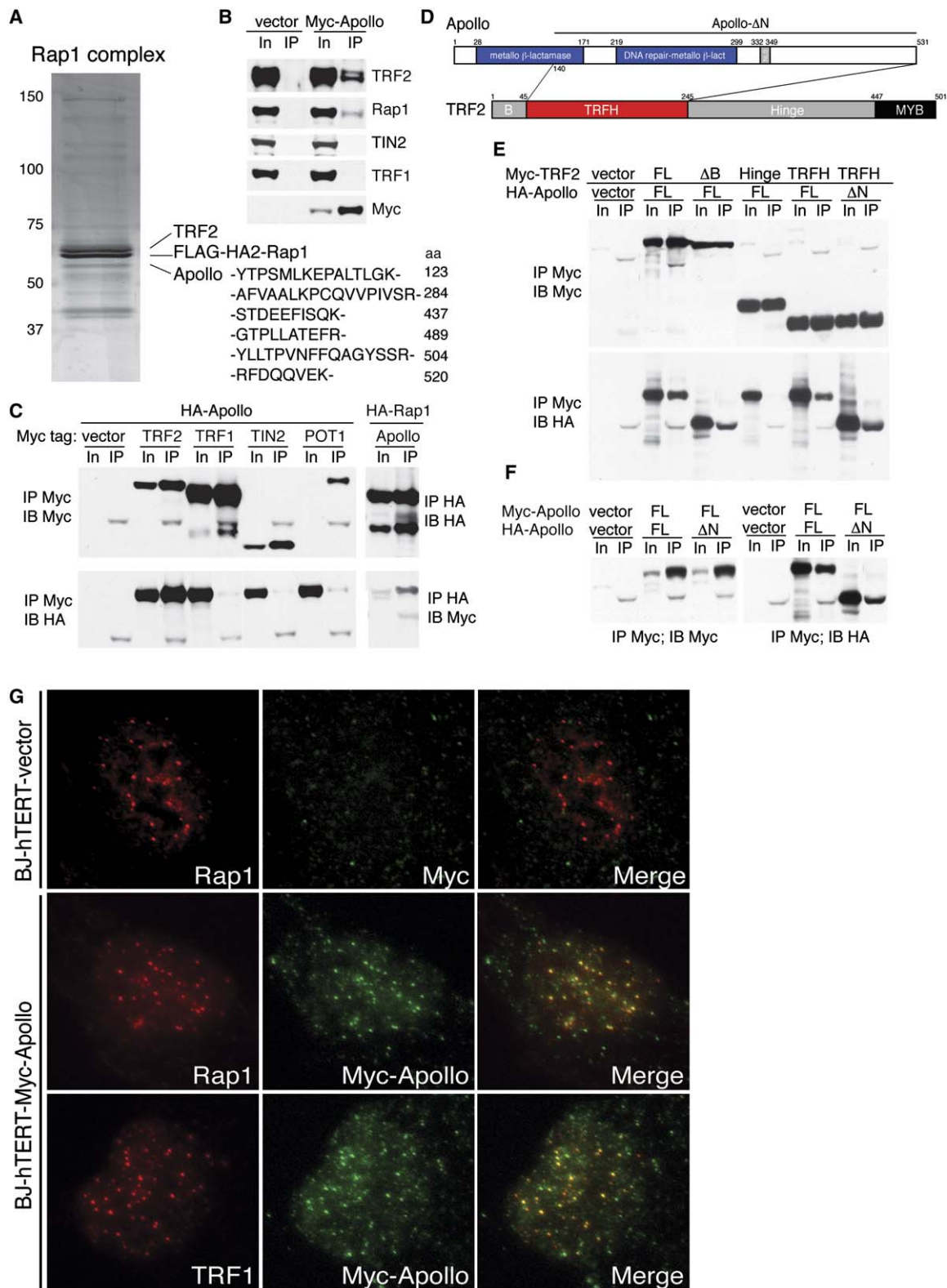*Correspondence: delange@rockefeller.edu

Figure 1. Identification of Apollo as a TRF2-Interacting Protein Associated with Shelterin and Telomeres

(A) Silver-stained gel of the Rap1 complex isolated with FLAG/HA affinity purification of a C-terminally tagged FLAG-[HA]2-Rap1 construct expressed in the human HeLa S3 clone. MWs are in kDa. The peptide sequences identifying SNM1B/Apollo were derived from the 60 kDa protein migrating below the TRF2/Rap1 doublet.

(B) Interaction of Apollo with endogenous TRF2 and Rap1, but not TIN2 or TRF1. 293T cells were transiently transfected with pLPC-Myc-Apollo, and immunoprecipitations (IP) were performed with the Myc antibody 9E10. IPs were analyzed by immunoblotting for the proteins indicated at

through an interaction with TRF2. We note that the data do not exclude the possibility that Apollo interacts with a shelterin subcomplex that lacks one or more of the core components. The interaction of SNM1B with TRF2 was recently reported by Freibaum and Counter [16].

To determine whether Apollo can associate with telomeres, we expressed Myc-tagged Apollo in hTERT-immortalized human BJ fibroblasts (BJ-hTERT) and determined its localization by indirect immunofluorescence (IF). Myc-tagged Apollo showed a homogeneous nuclear staining pattern (data not shown). Extraction of soluble nucleoplasmic proteins with Triton-X 100 revealed numerous small Myc-Apollo foci that coincided with TRF1 and Rap1 signals (Figure 1G), indicating that they represented telomeres. Myc-tagged Apollo was also found in small foci that did not colocalize with telomeric markers. The nature of these localization sites was not determined. In contrast to what has been reported for SNM1A, we did not observe a general relocalization of Myc-tagged Apollo to IR-induced sites of DNA damage (Figure S2). Attempts to detect the endogenous Apollo with an affinity-purified peptide antibody failed (data not shown). Because this α-Apollo antibody detected retrovirally expressed Apollo by IF (data not shown) and in immunoblots (Figure S1C), the failure to detect the endogenous protein is most likely due to its low abundance, which was noted previously [2, 4, 7]. Its low abundance at telomeres argues against Apollo's being a component of the shelterin core complex. Hence, Apollo appears to be one of the shelterin accessory factors that are present as low copy number at telomeres and/or have a transient association with chromosome ends.

Because several other shelterin-associated factors have been shown to play a role at telomeres, we used RNAi-mediated knockdown to determine whether Apollo also contributes to telomere function. Five independent shRNAs were found to effectively reduce the Apollo mRNA levels as determined by RT-PCR (Figure 2A; see Figure S1B for primer location). Two of the shRNAs were also tested for their ability to diminish the levels of Myc-tagged Apollo expressed from a retroviral construct (Figure S1C). Primary human IMR90 fibroblasts with diminished Apollo mRNA levels showed a clear growth defect (Figure 2B). Within a week of introduction of Apollo shRNAs, the cells gradually slowed their proliferation and appeared to arrest. The reduced proliferation was due to the depletion of Apollo because it was rescued by the coinfection with a retrovirus encoding a mutated version of Apollo lacking the target site for one of the shRNAs (Figure S3A). The arrested Apollo knockdown cells had a senescent morphology and expressed SA-β-galactosidase, a marker for cellular senescence (Figure 2C). In addition, all Apollo shRNAs induced the upregulation of the CDK inhibitor p21, a read-out for p53 activation (Figure 2D). Induction of p16, a second CDK inhibitor implicated in senescence, only occurred with Apollo shRNA H2 and may be an off-target effect (Figure 2D). Induction of senescence has previously been observed upon inhibition of TRF2 [17]. However, the Apollo shRNAs did not affect the levels of TRF2 and Rap1 protein (Figure 2E), arguing that the phenotypes are not due to diminished TRF2 function. Whereas the senescence phenotype was observed with five independent Apollo shRNAs in IMR90 and also occurred in BJ and hTERT-immortalized BJ fibroblasts (data not shown), no growth defect was observed upon introduction of the Apollo shRNAs in fibroblasts transformed with SV40 large T antigen or in the HeLa tumor cell line (data not shown). Further work will be required to determine whether Apollo is dispensable for the proliferation of such transformed cells.

The senescence resulting from Apollo knockdown is consistent with the cells experiencing a persistent DNA-damage signal. Dysfunctional telomeres are recognized by the canonical DNA-damage signaling pathway, leading to activation of the ATM kinase [18] and accumulation of DNA-damage response factors at chromosome ends [19, 20]. The resulting TIFs are a well-established read-out for telomere damage. Diminished Apollo expression enforced by three independent shRNAs resulted in TIFs in ~20% of IMR90 cells (Figure 3). The TIFs were obvious from IF for γ-H2AX and 53BP1 and the colocalization of these DNA-damage response factors with TRF1 (Figure 3A). The median number of TIFs per nucleus was ~12 (Figure 3C). The TIF phenotype associated with Apollo shRNA H6 was not observed if the cells coexpressed the version of Apollo resistant to this hairpin (Figure S3B), showing that the DNA-damage signal is the result of Apollo inhibition. Apollo knockdown also resulted in 53BP1 and γ-H2AX foci that were not obviously associated with telomeres, suggesting that Apollo is required for global genome integrity as well as telomere protection. However, more than half of the DNA-damage response foci in the Apollo knockdown were localized at chromosome ends (Figure 3D), indicating that Apollo deficiency preferentially affected telomeres.

---

the right, with the following antibodies (top to bottom): 647, 765, 864, 371, and 9E10. For panels (B), (D), (E), and (F), lanes marked "In" represent 2.5% of in the input lysate used for the IPs.

(C) Co-IP of Apollo with cotransfected TRF2 and Rap1. 293T cells were transiently transfected with the indicated pLPC constructs, and IPs were performed with the 9E10 Myc antibody (left) or an HA antibody (HA.11) (right). IPs were analyzed by immunoblotting (IB) for protein expression (top) and for interaction with Apollo (bottom), with the indicated antibodies.

(D) Schematic of the interaction between Apollo and TRF2. The following abbreviations are used: B, basic domain; TRFH, TRF homology domain; MYB, Myb-type DNA binding domain; and NLS, putative nuclear localization signal.

(E) Apollo interacts with the TRFH domain of TRF2. Myc IPs of extracts from 293T cells transfected with the indicated constructs were immunoblotted with the Myc antibody to detect the TRF2 alleles and the HA antibody to detect Apollo. The TRF2 domains referred to above the lanes (FL denotes full length) and the ΔN version of Apollo are shown in panel (D).

(F) Apollo interacts with itself. 293T cotransfection experiments were as in panels (C) and (E) with the indicated constructs. Antibodies used for IP and IB are indicated.

(G) Localization of retrovirally expressed Myc-tagged Apollo in BJ-hTERT cells. Apollo was detected by using the 9E10 Myc Ab (Alexa488, green). Rap1 was detected with Ab 765 (RRX, red). TRF1 was detected with Ab 371 (RRX, red). Cells were extracted with Triton-X 100 to remove soluble proteins. Top panels show BJ-hTERT cells infected with the empty pLPC vector.

A

Apollo shRNAs

Luc | H2 | H6 | H7 | H8 | UTR

Apollo

GAPDH

B

C

Luciferase

Apollo sh H6

Apollo sh H2

D

Apollo shRNAs

Luc | H2 | H6 | H7

p21

p16

γ-tub

E

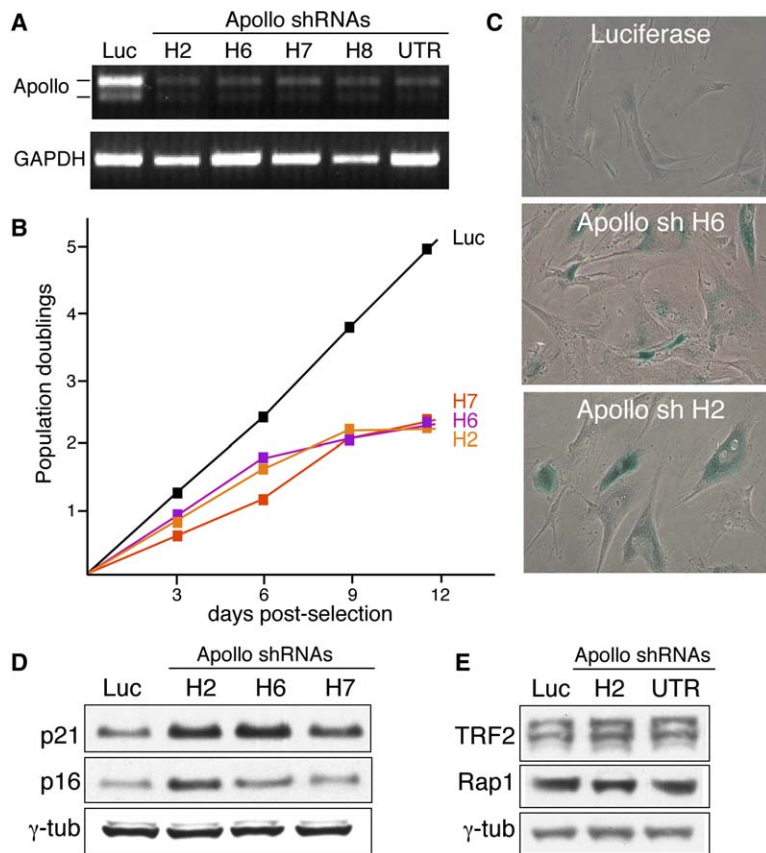Apollo shRNAs

Luc | H2 | UTR

TRF2

Rap1

γ-tub

Figure 2. Diminished Apollo Expression in Human IMR90 Fibroblasts Results in a Senescent-like Phenotype

(A) Reduction of Apollo mRNA levels resulting from RNAi. RNA derived from cells infected with the indicated shRNA-encoding retroviruses was processed to detect Apollo mRNA and GAPDH mRNA as a control with RT-PCR (see Experimental Procedures and Figure S1B). The RT-PCR detects two versions of Apollo mRNA generated by alternative splicing (Figure S1B). Luc denotes luciferase shRNA.

(B) Diminished cell proliferation upon inhibition of Apollo. IMR90 cells were infected with the indicated shRNA retroviruses and subjected to puromycin selection for 3 days. Subsequently, cells numbers were measured at the indicated time points, with day 0 representing the first day after puromycin selection.

(C) Senescence-like phenotype of IMR90 cells with diminished Apollo expression. Twelve days after selection for the indicated shRNAs, cells were photographed after staining (37°C, overnight) for SA-β-galactosidase [40].

(D) Induction of p21 upon Apollo inhibition. Immunoblot of extracts from the cells shown in (B) at day 5 after selection. The following antibodies were used: p21, F5 (Santa Cruz); p16, C20 (Santa Cruz); and γ-tubulin, GTU 488 (Sigma).

(E) Apollo knockdown does not affect TRF2 and Rap1. Immunoblot of extracts from the cells shown in (B) at day 5 after selection. The following antibodies were used: TRF2 (647); Rap1 (765); and γ-tubulin, GTU 488 (Sigma).

Because the TIFs were only observed in ~20% of the Apollo knockdown cells, we asked whether they appeared in a specific stage of the cell cycle. Initial experiments suggested that the TIFs arose during or after DNA replication. Specifically, we noted that the TIF-positive cells often had a subset of telomeric signals that appeared as doublets (Figure 3A). This pattern suggested that the TIFs occurred in cells that had replicated some, but not all, of their telomeres. To test whether the TIFs were more prominent in S phase than in G1, we examined cells that had been cultured in the presence of BrdU for 3 hr. Very few TIF-positive cells lacked the ability to incorporate BrdU (Figure 3E). The fraction of TIF-positive cells that had incorporated BrdU was 91% and 83% for the Apollo shRNAs H2 and UTR, respectively (n ≥ 150 for each). On the basis of the nuclear BrdU staining pattern, the TIF-positive cells appeared to be in all stages of S phase (data not shown). This would be expected if the TIFs are associated with telomere replication because mammalian telomeres replicate throughout S phase [21, 22]. Collectively, the data suggest that Apollo contributes to the protection of telomeres during or after DNA replication.

Because knockdown of Apollo induced a DNA-damage signal at telomeres, we evaluated the status of the telomeric DNA. DNA analysis showed no significant changes in the telomeric overhang or the double-stranded telomeric-repeat array (Figures S4A and S4B). In addition, the analysis of metaphase spreads

derived from Apollo knockdown cells did not show significant levels of telomere aberrations (Figure 4A and data not shown), including the previously described indices of telomere dysfunction such as telomere-telomere fusions [17], telomere sister-chromatid exchanges [23, 24], telomeric DNA-containing Double Minute chromosomes [25], or extrachromosomal telomeric signals [26]. However, we did observe a small but significant increase of chromatid ends with two or more distinct telomeric FISH signals instead of one (Figures 4A and 4B). Chromosome orientation FISH (CO-FISH; [27]) showed that there was no preference for the telomere generated by lagging-strand or leading-strand DNA synthesis with regard to the occurrence of these doublets (data not shown). Telomere doublets at single-chromatid ends have been noted previously in Atm−/− mouse cells [28] and also occur at low frequency in unperturbed human fibroblasts and other human cells (Figure 4B; [29]). The nature and origin of these aberrant telomere structures has not been established.

This study and the accompanying report from the Gilson group [30] identifies the Artemis-like nuclease Apollo as a telomere-associated factor. Although Apollo interacts with TRF2 and can be targeted to telomeres, our inability to detect the endogenous Apollo at chromosome ends suggests that it is much less abundant than shelterin. On the basis of its low abundance and the data suggesting that Apollo has a nontelomeric function in ICL repair, Apollo qualifies as a shelterin accessory
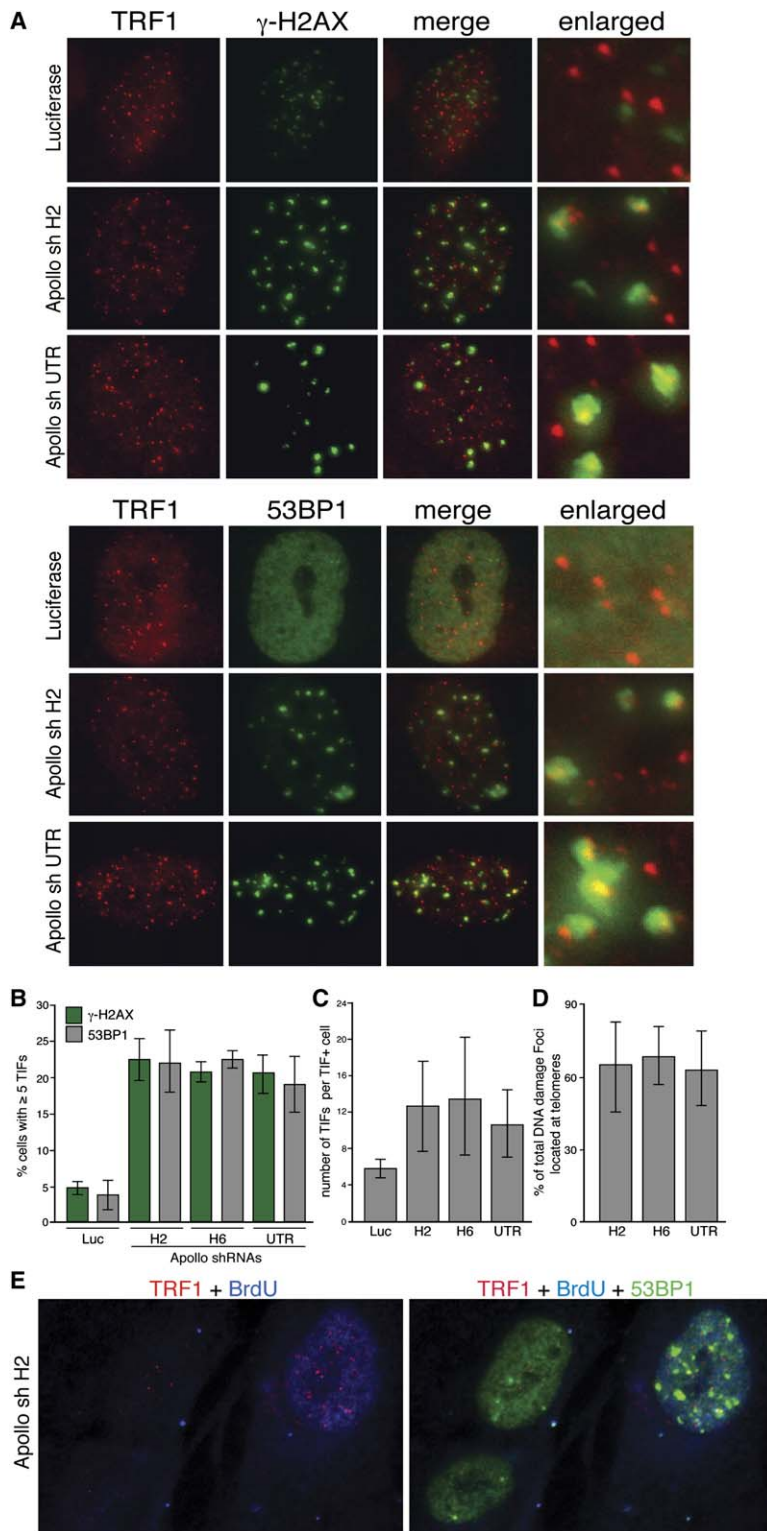
Figure 3. Induction of a Telomere Damage Signal in Cells with Diminished Apollo

(A) IF showing colocalization of γ-H2AX (top) and 53BP1 (bottom) foci with telomeric sites marked by TRF1 in IMR90 nuclei of cells treated with the Apollo shRNAs indicated on the left. The following antibodies were used: TRF1, 371 (RRX, red); γ-H2AX from Upstate (Alexa488, green); and 53BP1 Mab, a gift from T. Halazonetis (Alexa488, green). Cells were processed at day 3 after selection.

(B) Quantification of the induction of TIFs by Apollo shRNAs. Cells were processed as shown in panel (A), and TIFs were scored on the basis of colocalization of DNA-damage factors with TRF1. The bar graph shows the percentage of cells (median and standard deviation based on n = 3; >100 cells per data point) containing five or more TIFs for each of the indicated shRNAs.

(C) Quantification of the number of TIFs per cell. The bar graph represents data derived from images as shown in (A). The percentage of foci colocalizing with TRF1 was determined in nuclei with ≥5 TIFs.

(D) Quantitative analysis of the fraction of DNA-damage foci that colocalize with telomeres. Cells were processed as in (A) and (B). For each TIF-positive nucleus, the percentage of foci colocalizing with TRF1 was determined. Data from γ-H2AX and 53BP1 IF were indistinguishable and were pooled to generate the bar graphs.

(E) TIFs occur preferentially in S phase cells. IMR90 cells 4 days after introduction of Apollo shRNA H2 were cultured in the presence of BrdU for 3 hr and then processed for IF. The images show IF for TRF1, BrdU, and γ-H2AX as indicated. See Experimental Procedures. Antibodies for TRF1 and 53BP1 are as in (A). 91% of the TIF-positive cells contained BrdU (n = 173). A similar result was obtained for shRNA UTR.

factor rather than a bona fide component of the shelterin core complex. The shelterin accessory factors with known function in DNA-damage processing have been proposed to execute or regulate processing steps that are needed for telomere protection and/or maintenance [1]. However, the telomeric function of relatively few shelterin-associated proteins has been elucidated.

Examples are the multifunctional PARP; tankyrase 1, which plays a role in the regulation of telomere length [31, 32]; the WRN helicase, which contributes to telomere stability [33, 34]; and the NHEJ factor Ku, which represses homologous recombination at telomeres [35]. What distinguishes Apollo from these and other shelterin accessory factors is the prominent telomere
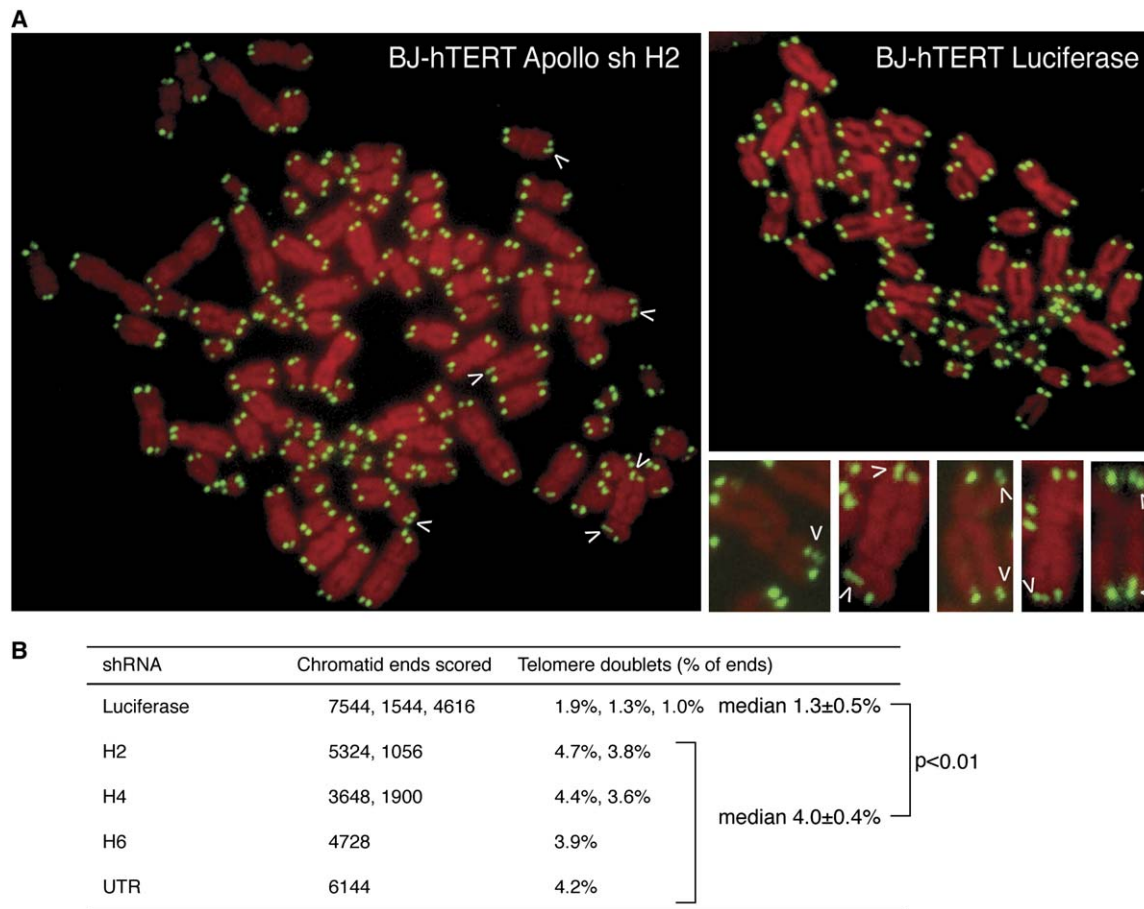
Figure 4. Apollo shRNAs Increase the Occurrence of Single-Chromatid Telomere Doublets

(A) Metaphase spreads illustrating presence of telomere doublets at single-chromatid ends. Metaphase spreads were obtained from BJ-hTERT cells treated with the indicated shRNAs and processed for telomeric FISH (FITC, green). DNA was stained with DAPI (false colored in red). Arrowheads highlight chromatids with telomere doublets. Enlarged images (bottom right) are derived from BJ-hTERT cells and BJ cells expressing SV40 large T antigen, both treated with Apollo shRNAs. Metaphases were harvested at day 3 after selection.

(B) Quantification of telomere doublets in BJ-hTERT cells treated with the indicated shRNAs. Metaphases were treated as in (A) and examined for the occurrence of telomere doublets at each chromatid end. p value was based on Student's t test. Data were derived from cells with and without SV40 large T. There was no significant difference between the two datasets.

DNA-damage signal resulting from its partial inhibition. Apollo appears to repress the DNA-damage signal at telomeres during or after their replication, and in its absence, a subset of the replicated telomeres attain features of DNA breaks and appear structurally aberrant in mitosis. Telomeres are thought to require multiple processing steps during and after DNA replication in order to regenerate the correct structure at the telomere terminus, to attain the protected state, and to allow telomerase-mediated telomere maintenance. It will be important to understand whether and how Apollo contributes to these events.

Experimental Procedures

Isolation of the Rap1 complex was performed by FLAG-HA affinity purification as described previously [3]. Eluted proteins were separated by SDS-PAGE (5%–15% gradient), the 60 kDa band was excised and subjected to trypsin digestion. The resulting peptides were extracted, and the protein was identified by mass spectrometry at the Rockefeller University Proteomics Resource Center. Apollo (SNM1B) cDNA was obtained from Invitrogen, and tagged versions of Apollo were generated by using standard PCR cloning into the pLPC retroviral vector. 293T cell transfection and immunoprecipitation were performed as described previously [3]. shRNAs were generated in pSUPER-retro (OligoEngine), and retroviral infections were performed as described previously [36]. The sequences of the shRNA targets are as follows: H2, 5′-GAAGCTGCCCACCAGATTG-3′; H6, 5′-GACTCTGTACAGCAATACA-3′; H7, 5′-GATCAATCTCAAG CTGACA-3′; H8, 5′-GATGGAGGTCCAGAAGCCA-3′; and UTR, 5′-GGTCCTCGTGCCTATGGAA-3′. The Luciferase control hairpin is 5′-CGTACGCGGAATACTTCGA-3′. The target sequence of shRNA H6 was changed to 5′-GACTCCGTCCAACAATACA-3′ by standard site-directed mutagenesis to create pLPC-Myc Apollo*H6. RT-PCR was performed with the oligo-dT ThermoScript RT-PCR system (Invitrogen). RNA was isolated from approximately 10^6 cells with the Qiagen RNAeasy kit. Three to four micrograms RNA was reverse transcribed with the ThermoScript RT-PCR system (Invitrogen) by using oligo dT priming and the protocol provided by the manufacturer. The primers used for PCR after cDNA synthesis are as follows: Apollo RT1 (forward GACTCCAACCCTACCACCATGAATG, reverse CAGTAGCTGTACCAACTCCAGGCGC) and GAPDH (forward TGAA GGTCGGAGTCAACGGATTTGGT, reverse CATGTGGGCCATGAGG TCCACCAC). Antibody to a KLH-conjugated Apollo peptide (NH$_2$-SRKIHSSHPDIHVIPYSDHSSYSC-COOH; starting at aa 259) was generated in NZW rabbits (Covance). The resulting immune serum, Ab 1477, was affinity purified. Procedures for immunoblotting,

indirect immunofluorescence, analysis of telomeric DNA, and metaphase chromosomes have been described previously [3, 37–39]. For the analysis of the cell-cycle stage of TIF induction, IMR90 cells were pulsed with 10 μM BrdU for 3 hr, fixed in 3% paraformaldehyde, and stained first for TRF1 and 53BP1 and then with rabbit-RRX (Jackson), mouse-Cy5 (Molecular Probes), and rat anti-BrdU conjugated to FITC (AxyII) in a buffer containing 10% goat serum, 3 mM MgCl2, and 100 U/ml DNaseI.

Supplemental Data

Supplemental Data include four figures and are available with this article online at: http://www.current-biology.com/cgi/content/full/16/13/1295/DC1/.

References

1. de Lange, T. (2005). Shelterin: The protein complex that shapes and safeguards human telomeres. Genes Dev. *19*, 2100–2110.
2. Moshous, D., Callebaut, I., de Chasseval, R., Corneo, B., Cavazzana-Calvo, M., Le Deist, F., Tezcan, I., Sanal, O., Bertrand, Y., Philippe, N., et al. (2001). Artemis, a novel DNA double-strand break repair/V(D)J recombination protein, is mutated in human severe combined immune deficiency. Cell *105*, 177–186.
3. Ye, J.Z., Donigian, J.R., Van Overbeek, M., Loayza, D., Luo, Y., Krutchinsky, A.N., Chait, B.T., and de Lange, T. (2004). TIN2 binds TRF1 and TRF2 simultaneously and stabilizes the TRF2 complex on telomeres. J. Biol. Chem. *279*, 47264–47271.
4. Dronkert, M.L., de Wit, J., Boeve, M., Vasconcelos, M.L., van Steeg, H., Tan, T.L., Hoeijmakers, J.H., and Kanaar, R. (2000). Disruption of mouse SNM1 causes increased sensitivity to the DNA interstrand cross-linking agent mitomycin C. Mol. Cell. Biol. *20*, 4553–4561.
5. Callebaut, I., Moshous, D., Mornon, J.P., and de Villartay, J.P. (2002). Metallo-beta-lactamase fold within nucleic acids processing enzymes: The beta-CASP family. Nucleic Acids Res. *30*, 3592–3601.
6. Poinsignon, C., Moshous, D., Callebaut, I., de Chasseval, R., Villey, I., and de Villartay, J.P. (2004). The metallo-beta-lactamase/beta-CASP domain of Artemis constitutes the catalytic core for V(D)J recombination. J. Exp. Med. *199*, 315–321.
7. Demuth, I., Digweed, M., and Concannon, P. (2004). Human SNM1B is required for normal cellular response to both DNA interstrand crosslink-inducing agents and ionizing radiation. Oncogene *23*, 8611–8618.
8. Richie, C.T., Peterson, C., Lu, T., Hittelman, W.N., Carpenter, P.B., and Legerski, R.J. (2002). hSnm1 colocalizes and physically associates with 53BP1 before and after DNA damage. Mol. Cell. Biol. *22*, 8635–8647.
9. Ma, Y., Pannicke, U., Schwarz, K., and Lieber, M.R. (2002). Hairpin opening and overhang processing by an Artemis/DNA-dependent protein kinase complex in nonhomologous end joining and V(D)J recombination. Cell *108*, 781–794.
10. Rooney, S., Sekiguchi, J., Zhu, C., Cheng, H.L., Manis, J., Whitlow, S., DeVido, J., Foy, D., Chaudhuri, J., Lombard, D., et al. (2002). Leaky Scid phenotype associated with defective V(D)J coding end processing in Artemis-deficient mice. Mol. Cell *10*, 1379–1390.
11. Riballo, E., Kuhne, M., Rief, N., Doherty, A., Smith, G.C., Recio, M.J., Reis, C., Dahm, K., Fricke, A., Krempler, A., et al. (2004). A pathway of double-strand break rejoining dependent upon ATM, Artemis, and proteins locating to gamma-H2AX foci. Mol. Cell *16*, 715–724.
12. Rooney, S., Alt, F.W., Lombard, D., Whitlow, S., Eckersdorff, M., Fleming, J., Fugmann, S., Ferguson, D.O., Schatz, D.G., and Sekiguchi, J. (2003). Defective DNA repair and increased genomic instability in Artemis-deficient murine cells. J. Exp. Med. *197*, 553–565.
13. Broccoli, D., Chong, L., Oelmann, S., Fernald, A.A., Marziliano, N., van Steensel, B., Kipling, D., Le Beau, M.M., and de Lange, T. (1997). Comparison of the human and mouse genes encoding the telomeric protein, TRF1: Chromosomal localization, expression and conserved protein domains. Hum. Mol. Genet. *6*, 69–76.
14. Fairall, L., Chapman, L., Moss, H., de Lange, T., and Rhodes, D. (2001). Structure of the TRFH dimerization domain of the human telomeric proteins TRF1 and TRF2. Mol. Cell *8*, 351–361.
15. Li, B., Oestreich, S., and de Lange, T. (2000). Identification of human Rap1: Implications for telomere evolution. Cell *101*, 471–483.
16. Freibaum, B.D., and Counter, C.M. (2006). hSnm1B is a novel telomere-associated protein. J. Biol. Chem., in press. Published online April 10, 2006. 10.1074/jbc.C600038200.
17. van Steensel, B., Smogorzewska, A., and de Lange, T. (1998). TRF2 protects human telomeres from end-to-end fusions. Cell *92*, 401–413.
18. Karlseder, J., Broccoli, D., Dai, Y., Hardy, S., and de Lange, T. (1999). p53- and ATM-dependent apoptosis induced by telomeres lacking TRF2. Science *283*, 1321–1325.
19. d'Adda di Fagagna, F., Reaper, P.M., Clay-Farrace, L., Fiegler, H., Carr, P., Von Zglinicki, T., Saretzki, G., Carter, N.P., and Jackson, S.P. (2003). A DNA damage checkpoint response in telomere-initiated senescence. Nature *426*, 194–198.
20. Takai, H., Smogorzewska, A., and de Lange, T. (2003). DNA damage foci at dysfunctional telomeres. Curr. Biol. *13*, 1549–1556.
21. Ten Hagen, K.G., Gilbert, D.M., Willard, H.F., and Cohen, S.N. (1990). Replication timing of DNA sequences associated with human centromeres and telomeres. Mol. Cell. Biol. *10*, 6348–6355.
22. Wright, W.E., Tesmer, V.M., Liao, M.L., and Shay, J.W. (1999). Normal human telomeres are not late replicating. Exp. Cell Res. *251*, 492–499.
23. Bailey, S.M., Brenneman, M.A., and Goodwin, E.H. (2004). Frequent recombination in telomeric DNA may extend the proliferative life of telomerase-negative cells. Nucleic Acids Res. *32*, 3743–3751.
24. Bechter, O.E., Shay, J.W., and Wright, W.E. (2004). The frequency of homologous recombination in human ALT cells. Cell Cycle *3*, 547–549, Published online May 10, 2004.
25. Zhu, X.D., Niedernhofer, L., Kuster, B., Mann, M., Hoeijmakers, J.H., and de Lange, T. (2003). ERCC1/XPF removes the 3′ overhang from uncapped telomeres and represses formation of telomeric DNA-containing double minute chromosomes. Mol. Cell *12*, 1489–1498.
26. Hande, M.P., Balajee, A.S., Tchirkov, A., Wynshaw-Boris, A., and Lansdorp, P.M. (2001). Extra-chromosomal telomeric DNA in cells from Atm(−/−) mice and patients with ataxia-telangiectasia. Hum. Mol. Genet. *10*, 519–528.
27. Bailey, S.M., Cornforth, M.N., Kurimasa, A., Chen, D.J., and Goodwin, E.H. (2001). Strand-specific postreplicative processing of mammalian telomeres. Science *293*, 2462–2465.
28. Undarmaa, B., Kodama, S., Suzuki, K., Niwa, O., and Watanabe, M. (2004). X-ray-induced telomeric instability in Atm-deficient mouse cells. Biochem. Biophys. Res. Commun. *315*, 51–58.
29. Philippe, C., Coullin, P., and Bernheim, A. (1999). Double telomeric signals on single chromatids revealed by FISH and PRINS. Ann. Genet. *42*, 202–209.
30. Lenain, C., Bauwens, S., Amiard, S., Brunori, M., Giraud-Panis, M.-J., and Gilson, E. (2006). The Apollo 5′ exonuclease functions together with TRF2 to protect telomeres from DNA repair. Curr.

Biol. *16*, in press. Published online May 25, 2006. 10.1016/j.cub.2006.05.021.

31. Smith, S., and de Lange, T. (2000). Tankyrase promotes telomere elongation in human cells. Curr. Biol. *10*, 1299–1302.

32. Smith, S., Giriat, I., Schmitt, A., and de Lange, T. (1998). Tankyrase, a poly(ADP-ribose) polymerase at human telomeres. Science *282*, 1484–1487.

33. Bai, Y., and Murnane, J.P. (2003). Telomere instability in a human tumor cell line expressing a dominant-negative WRN protein. Hum. Genet. *113*, 337–347.

34. Crabbe, L., Verdun, R.E., Haggblom, C.I., and Karlseder, J. (2004). Defective telomere lagging strand synthesis in cells lacking WRN helicase activity. Science *306*, 1951–1953.

35. Celli, G.B., Lazzerini Denchi, E., and de Lange, T. (2006). Ku70 stimulates fusion of dysfunctional telomeres yet protects chromosome ends from homologous recombination. Nat. Cell Biol., in press.

36. Karlseder, J., Smogorzewska, A., and de Lange, T. (2002). Senescence induced by altered telomere state, not telomere loss. Science *295*, 2446–2449.

37. Hockemeyer, D., Sfeir, A.J., Shay, J.W., Wright, W.E., and de Lange, T. (2005). POT1 protects telomeres from a transient DNA damage response and determines how human chromosomes end. EMBO J. *24*, 2667–2678.

38. Wang, R.C., Smogorzewska, A., and de Lange, T. (2004). Homologous recombination generates T-loop-sized deletions at human telomeres. Cell *119*, 355–368.

39. Ye, J.Z., Hockemeyer, D., Krutchinsky, A.N., Loayza, D., Hooper, S.M., Chait, B.T., and de Lange, T. (2004). POT1-interacting protein PIP1: A telomere length regulator that recruits POT1 to the TIN2/TRF1 complex. Genes Dev. *18*, 1649–1654.

40. Dimri, G.P., Lee, X., Basile, G., Acosta, M., Scott, G., Roskelley, C., Medrano, E.E., Linskens, M., Rubelj, I., Pereira-Smith, O., et al. (1995). A biomarker that identifies senescent human cells in culture and in aging skin in vivo. Proc. Natl. Acad. Sci. USA *92*, 9363–9367.

Supplemental Data

Apollo, an Artemis-Related Nuclease, Interacts with TRF2 and Protects Human Telomeres in S Phase
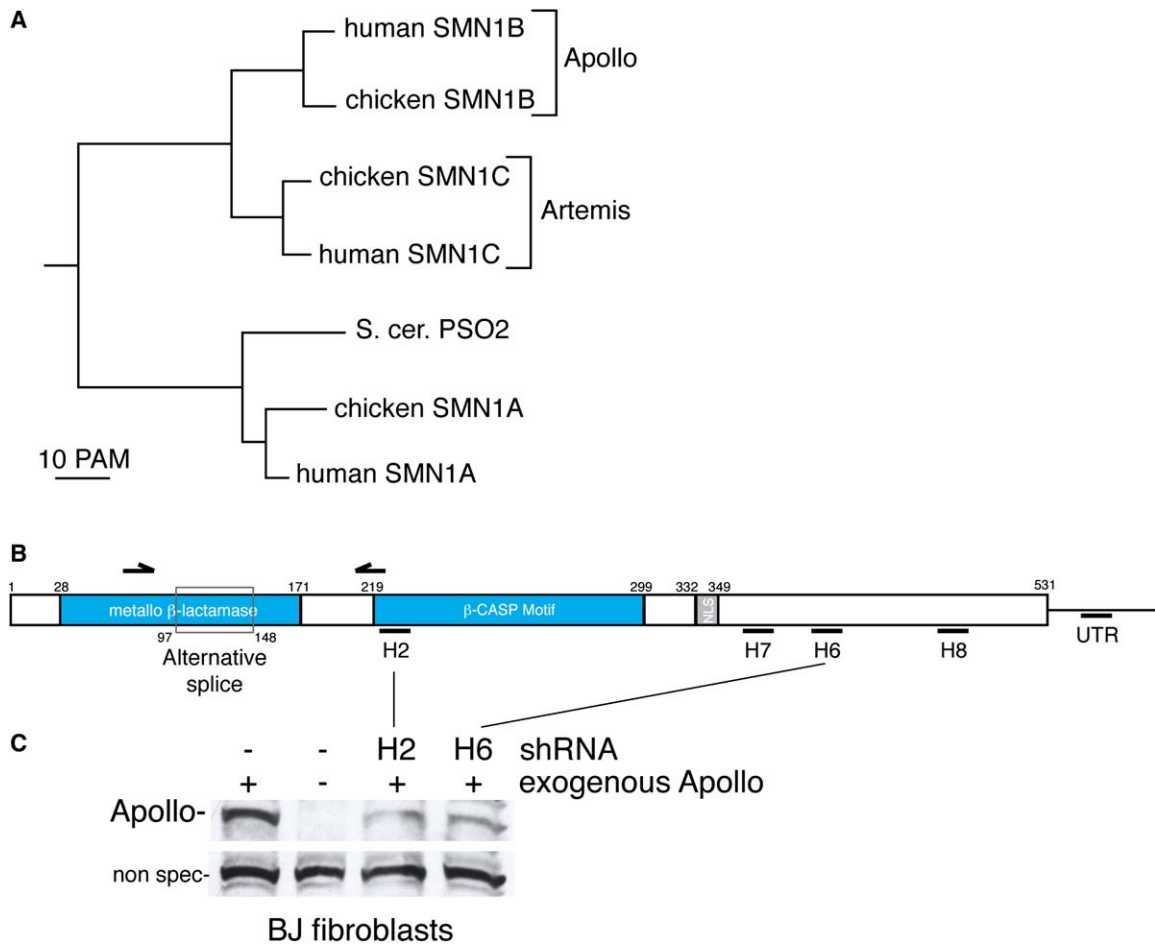
Megan van Overbeek and Titia de Lange

Figure S1. Naming, Structure, Detection, and Inhibition of Apollo

(A) Phylogenetic tree showing that Artemis and Apollo (SNM1B) are closely related. Protein sequences were obtained from the NCBI, and alignments were generated with CLUSTALW by using the Multalin website (http://prodes.toulouse.inra.fr/multalin/) with default setting for all parameters.

(B) Schematic of Apollo indicating the PCR primers used for RT-PCR and the target sites of the shRNA hairpins used for Apollo knockdown. The RT-PCR strategy detects Apollo mRNA with and without inclusion of the indicated alternatively spliced exon.

(C) Immunoblot showing reduced expression of exogenous Apollo upon introduction of Apollo shRNAs H2 and H6. BJ cells were infected with a retrovirus expressing Apollo or the empty vector and subsequently infected with the indicated shRNA retroviruses. An antibody raised to an Apollo peptide (Ab 1477) was used to detect the overexpressed protein. This antibody did not detect endogenous Apollo in immunoblots or by IF.
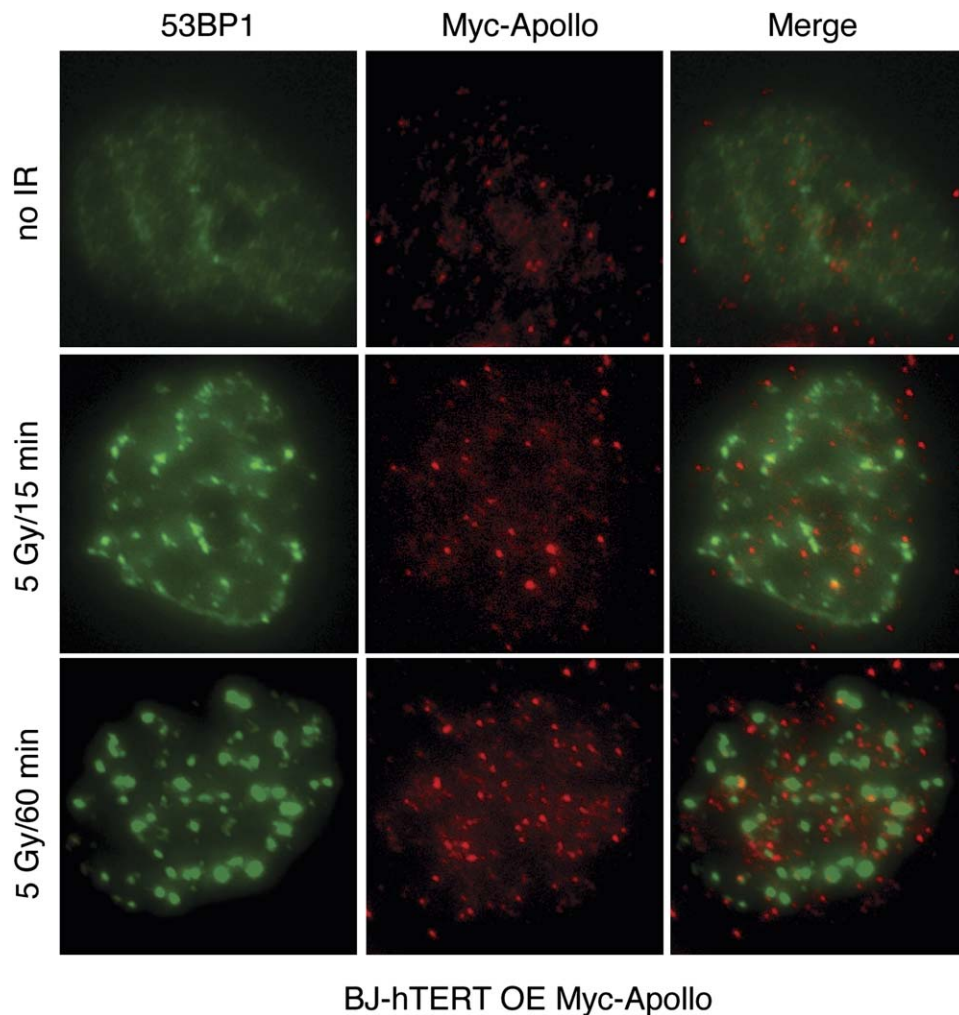
53BP1   Myc-Apollo   Merge

no IR

5 Gy/15 min

5 Gy/60 min

BJ-hTERT OE Myc-Apollo

Figure S2. Exogenously Expressed Apollo Does Not Localize at IR-Induced Foci

BJ-hTERT cells expressing Myc-tagged Apollo were irradiated as indicated and processed for IF at the indicated times. 53BP1 (Alexa488, green) was used as an indicator of DNA-damage foci. Apollo was detected with the 9E10 Myc antibody (RRX, red). Cells were pre-extracted with Triton-X 100. There was no significant change in the localization pattern of Apollo after IR, and the 53BP1 foci rarely colocalized with Apollo.
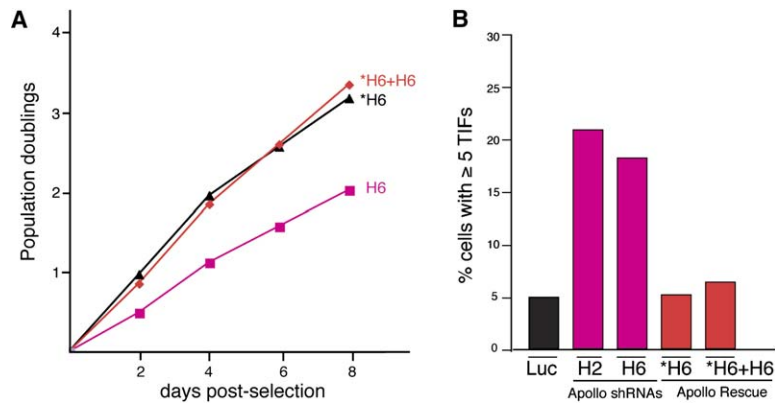
A

B

Figure S3. Rescue of the Growth Defect and TIF Phenotypes in Apollo Knockdown Cells by Coexpression of an shRNA-Resistant Apollo Allele

(A) Absence of the proliferation phenotype of Apollo shRNA H6 in cells that coexpress shRNA-resistant Apollo (*H6). BJ cells were infected with the indicated shRNA retroviruses and subjected to puromycin selection for 3 days. Subsequently, cell numbers were measured at the indicated time points, with day 0 representing the first day after puromycin selection.

(B) Absence of the TIF phenotype of Apollo shRNA H6 in cells coexpressing shRNA-resistant Apollo (*H6). BJ cells were processed as shown in Figure 3A, and nuclei were inspected for TIFs on the basis of colocalization of γ-H2AX with TRF1. The bar graph shows the percentage of cells containing five or more TIFs for each of the indicated cell lines.

A

native   denatured

B

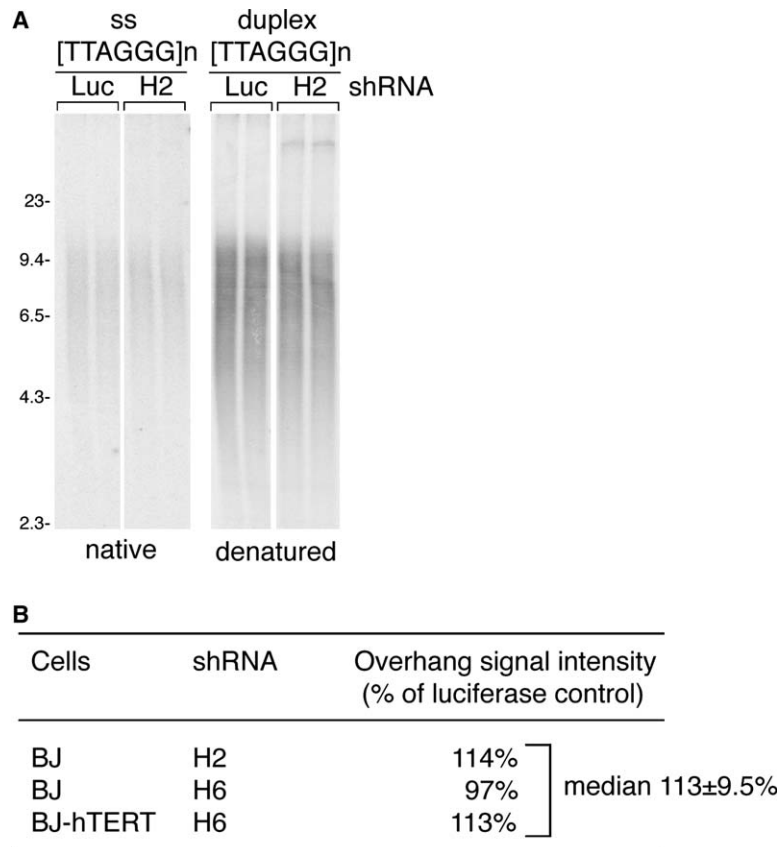| Cells	shRNA	Overhang signal intensity (% of luciferase control)	
BJ	H2	114%	
BJ	H6	97%	median 113±9.5%
BJ-hTERT	H6	113%	

Figure S4. Lack of Detectable Changes in the Telomeric DNA after Knockdown of Apollo with shRNAs

(A) Example of analysis of telomeric DNA. BJ cells infected with a retrovirus expressing shRNA H2 or the luciferase shRNA control were processed for DNA analysis 5 days after infection. DNA was harvested and digested with MboI/AluI and fractionated on an agarose gel. The single-stranded telomeric overhang was detected by in-gel hybridization of a ^{32}P-labeled C strand oligo. After quantification of the signal, the DNA was denatured in situ with NaOH, neutralized, and rehybridized with the same probe to detect the total telomeric DNA. The overhang signal was normalized to the total telomeric DNA in the same lane. These values were compared between cells containing the Apollo shRNA and the luciferase control. Molecular weights of the markers (to the left of the gel) are given in kb.

(B) Quantification of the relative overhang signal in Apollo knockdown cells. Cells (as indicated) infected with the listed Apollo shRNAs were analyzed as in (A) alongside the appropriate luciferase controls. The overhang signals were normalized to the total telomeric DNA signal, and these values were compared to the luciferase control in each experiment.